Progress In Electromagnetics Research Letters, Vol. 71, 97–102, 2017

A Dual-Band Slotted Square Ring Patch Antenna for Local Hyperthermia Applications

Hemn Younesiraad*, Mohammad Bemani, and Saeid Nikmehr

Abstract—In this paper, a simple dual-band compact slotted square ring patch antenna has been used as hyperthermia applicators in the treatment of cancerous human cells at superficial depths inside the body. The proposed antenna has the advantages of dual-band ($f_1 = 434\,\text{MHz}$ and $f_2 = 915\,\text{MHz}$) operation and more compact size ($124 \times 124\,\text{mm}^2$) than the current state-of-the-art designs without significant frequency detuning or impedance mismatch which makes it a more suitable choice for local hyperthermia. The proposed antenna provides a suitable specific absorption rate (SAR) penetration profile and shows a good resonance at two designed frequencies. We have optimized the structure so that the SAR level performed by the structure is sufficiently enough so as to meet the IEEE standard requirements for medical applications including hyperthermia. We have simulated and measured the structure with a low-profile substrate (i.e., FR4 substrate with $\varepsilon_r = 4.4$ and thickness of 1.6 mm). During the design process, the simplified planar tri-layered tissue model interfaced with a water bolus was used to incorporate the main electrical effects on the antenna. The results validate the proposed antenna design.

1. INTRODUCTION

Hyperthermia is a type of cancer treatment in which body tissue is exposed to high temperatures. In this therapy, temperature of the regions of the body with cancerous tumor-masses are raised over 41–42°C by non-invasively deploying electromagnetic radiation (energy), namely using a properly designed antenna. Several methods of hyperthermia are currently under study, including local, regional, and whole-body hyperthermia. In local hyperthermia, heat is applied to a small area, such as a tumor, using various techniques that deliver energy to heat the tumor. Different types of energy may be used to apply heat, including microwave, radiofrequency and ultrasound [1, 2]. The human basal metabolic rate is above 1 W/kg. One of the methods for superficial hyperthermia is using different types of applicators [3, 4]. Fig. 1 depicts a typical hyperthermia system in which electromagnetic energy coupling between the applicator and the body's tissue is carried out through water bolus. Also, the standard frequency bands for the hyperthermia applications are 27 MHz, 434 MHz, 915 MHz and the 2450 MHz [5–7] frequencies which all lie in the ISM bands.

One of the worthwhile antennas for the hyperthermia applications is the microstrip antenna. The main challenge in designing such antennas is to investigate the electrical characterization of the biological tissues of the body, such as their relative permittivity and conductance so as to include them in the design process. Moreover, the effects of the voxel size and the densities of the involved tissues on the electromagnetic characterization of the antenna should also be considered [8].

Regarding the conducted researches, it is shown that the dominant effects of the body's tissue on the performance of the antenna are due to three types of tissues, namely skin, fat and muscle. This result has been utilized to develop a tri-layered tissue model so as to include the electromagnetic effects that the tissue has on the antenna [9]. Finally, the design of the antenna can be carried out

Received 5 September 2017, Accepted 18 October 2017, Scheduled 2 November 2017
* Corresponding author: Hemn Younesiraad (younesiraad@tabrizu.ac.ir).
The authors are with the Department of Electrical and Computer Engineering, University of Tabriz, Tabriz, Iran.

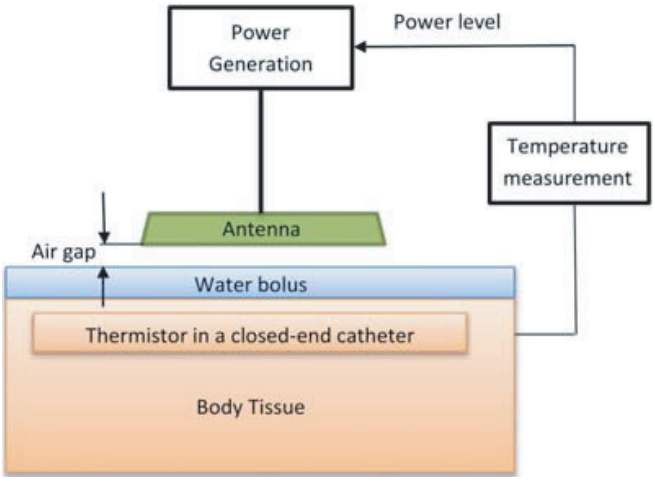

Figure 1. Schematic of local hyperthermia system.

using different numerical approaches such as finite-difference time-domain, Green's functions and finite element method or commercial software namely HFSS.

In this paper, a novel dual-band microstrip antenna has been proposed and designed to operate at two frequencies of $f_1 = 434\,\text{MHz}$ and $f_2 = 915\,\text{MHz}$. The proposed antenna has a simple structure and compact size. Hence, it could be a proper candidate for superficial hyperthermia applications. In the design process of the antenna, we have taken into account all of its design considerations which have helped us to fully optimize its electromagnetic properties. Electromagnetic characterizations of the antenna such as its return loss and SAR distribution are satisfactory.

2. ANTENNA DESIGN

Figure 2 depicts the topology of the proposed antenna. The proposed antenna consists of a square ring with a square patch inside the ring mounted on a low-profile FR4 substrate with $\varepsilon_r = 4.4$, $\tan\delta = 0.002$ and a thickness of $h = 1.6\,\text{mm}$. The antenna is fed through a $50\,\Omega$ coaxial cable placed at $(x, y) = (-47.68\,\text{mm}, -47.68\,\text{mm})$. We have employed a via at the top right corner of the square ring at $(x, y) = (36.18\,\text{mm}, 47.68\,\text{mm})$ with a radius of 0.5 mm. This helps us achieve a dual-band and more compact antenna. Also, the slotted ground is helpful not only in terms of improving the antenna gain and the antenna bandwidth, but also adjusting the resonating frequencies of the structure. Also, current distribution over the patch shows that in the proposed antenna, TM_{21} and TM_{01} modes are excited at the higher and lower frequencies, respectively, which makes the proposed antenna a proper choice for dual-band applications. Moreover, using the square patch helps further adjust the bandwidth. At last, the dimension of the proposed antenna is $124 \times 124 \times 1.6\,\text{mm}^3$ which enjoys a more compact size than the previous designs.

For the initial design of the antenna, we have used relations regarding the rectangular patches and their corresponding transmission line models [10]. After designing the square patch we set the initial dimensions of the square ring in the initial design of the antenna. Then, in the next step toward designing the geometric dimensions of the antenna, feeding port and via position were introduced as numerical parameters and were optimized using the HFSS software optimization toolbox to gain simultaneously proper return loss at two designed frequencies and suitable SAR distribution in the tri-layered based on the IEEE standards for local hyperthermia applications. The proposed antenna is designed to operate at two frequencies of $f_1 = 434\,\text{MHz}$ and $f_2 = 915\,\text{MHz}$ for hyperthermia applications. Throughout the design procedure and simulation of the antenna, we have adopted the tri-layered biological tissue model to incorporate the electromagnetic characterization of the human tissue [5]. The designed antenna was placed 2 mm away from the water bolus. Table 1 lists the conductivity, permittivity and the density of the biological human tissue at frequencies of $f_1 = 434\,\text{MHz}$ and $f_2 = 915\,\text{MHz}$. Data obtained from this table are imported into the HFSS software based on which the antenna design and simulation were performed. The final dimensions of the antenna are shown in Table 2.

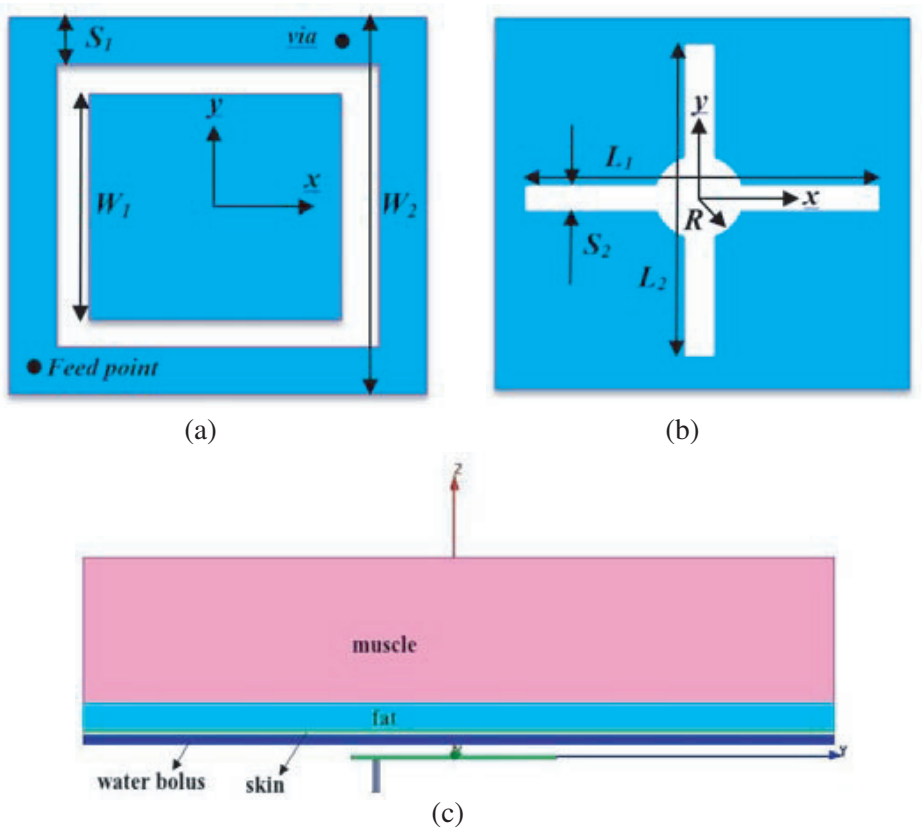

Figure 2. Proposed compact square ring patch antenna: (a) the front square ring/patch surface, (b) the rear ground plane/slots surface, (c) the tri-layered model tissue, water bolus and the antenna in HFSS.

Table 1. Permittivity, conductivity, density and thickness of the tissue material at $f_1 = 434\,\text{MHz}$ and $f_2 = 915\,\text{MHz}$.

Material	Permittivity (ε_r)		Conductivity ($\sigma \frac{s}{m}$)		Density $\rho(\frac{\text{kg}}{\text{m}^3})$	Phantom tissue layer thickness (mm)
	f_1	f_2	f_1	f_2		
De-ionized water	76.00	71.00	0.001	0.003	1000	5.0
Skin (dry)	46.05	41.33	0.702	0.872	1100	2.6
Fat (not infiltrated)	5.56	5.46	0.041	0.051	916	15.0
Muscle (transverse fiber)	56.86	54.99	0.805	0.948	1041	82.4

Table 2. Final geometric dimensions of the antenna (unit: millimeter).

W_1	W_2	S_1	S_2	L_1	L_2	R
70.93	104.48	9.11	3.83	113	101.6	9.58

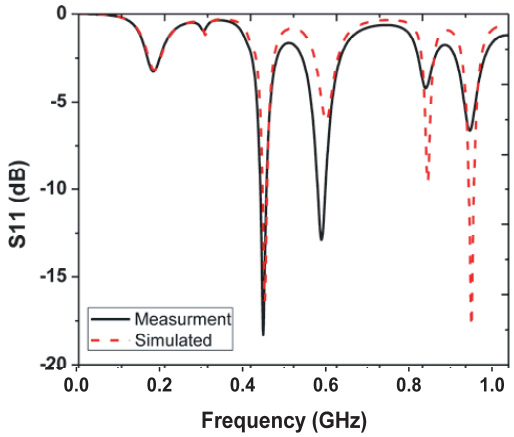

Figure 3. Simulated and measured return losses related to the proposed antenna.

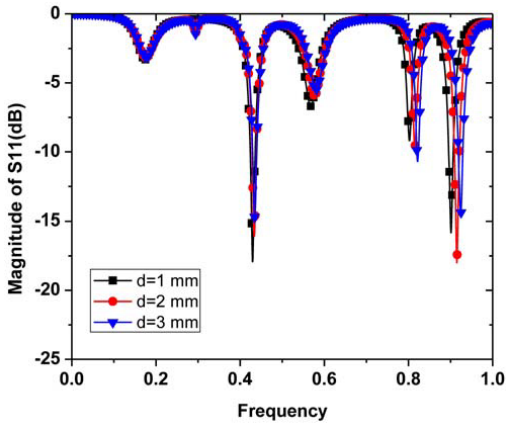

Figure 4. The effect of various air gaps on the return loss of the proposed antenna.

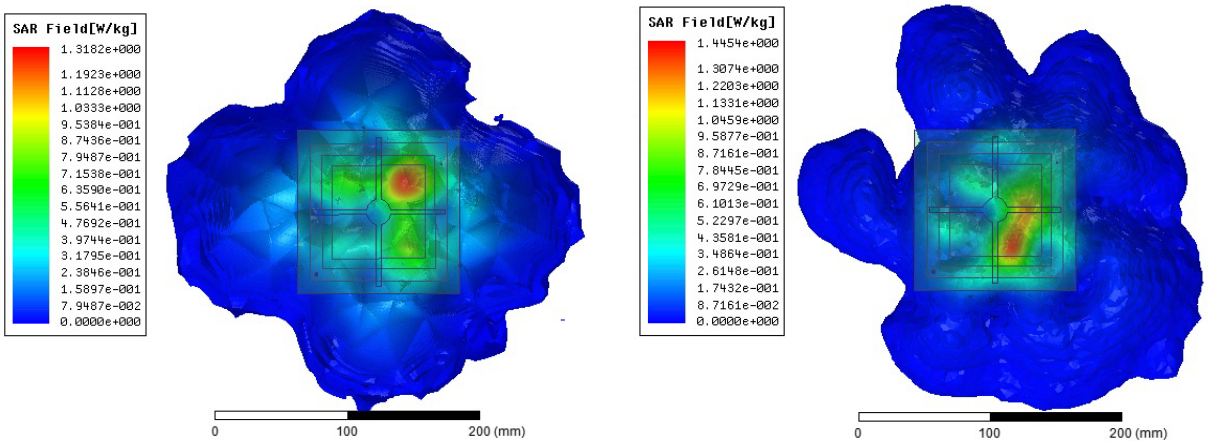

(a) (b)

Figure 5. Simulated SAR distribution in depth of 1 cm inside the muscle layer at (a) 434 MHz, (b) 915 MHz.

3. RESULTS AND DISCUSSION

Simulated and measured return losses of the propose antenna are illustrated in Fig. 3. As shown in Fig. 3, the return loss magnitudes of the proposed antenna are 16 dB and 17 dB at 434 MHz and 915 MHz, respectively. Bandwidths of 9 MHz (428–437 MHz) and 13 MHz (907–920 MHz) are achieved in $f_1 = 434$ MHz and $f_2 = 915$ MHz respectively. Therefore, the proposed antenna is suitable for local hyperthermia applications based on IEEE standards. The resonant characteristics of the proposed antenna were measured in free space and in the vicinity of muscle phantom simulating fluid, which was made from the recipes in [11]. In the simulation setup, we consider the tri-layered tissue model while in the measurement setup, we use only the simulated muscle phantom liquid to calculate the return loss. Therefore, the difference between simulation and measurement results is evident due to the effect of the electrical characteristics of the used tissues in both simulation and measurement setup. Fig. 4 shows the effect of various air gaps as well as uneven air gap on the antenna performance. As shown in Fig. 4, the impedance matching of the proposed antenna resonant frequency remains significantly and sufficiently stable, especially in the 434 MHz band, when the separation distance is changed. The resonant frequencies of the antenna are adjusted by coupling resonant currents on the dimensions of the square patch and the outer square ring. The orthogonal ground plane slots interrupt the resonant currents on the square patch and the outer square ring to reduce the overall patch dimensions.

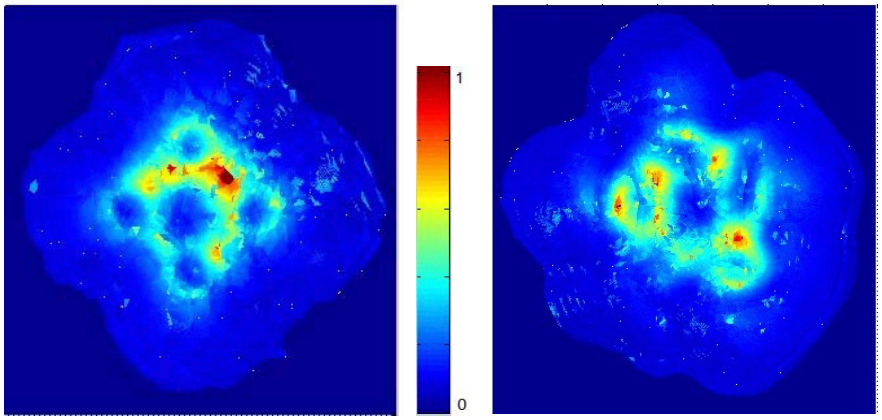

(a) (b)

Figure 6. Normalized measured SAR distribution at 1 cm inside the simulated muscle phantom liquid for the proposed antenna at (a) 434 MHz, (b) 915 MHz.

Table 3. Comparison of electromagnetic characteristics of the proposed antenna and previous works.

	This work		**[12]**		**[13]**	
Frequency (MHz)	$f_1 = 434$ MHz	$f_2 = 915$ MHz	$f_1 = 434$ MHz	$f_2 = 850$ MHz	$f_1 = 915$ MHz	$f_2 = 2450$ MHz
Return Loss (dB)	-16	-17	-28	-26	-32	-27
Peak SAR [W/kg]	1.32	1.44	0.15	0.15	11.17	27.93
Measured Peak SAR [W/kg]	4.97	5.14	Not available		Not available	
Size (mm^2)	124×124		50×35		120×120	

When the antenna was assumed to deliver 1 W, the 1-g averaged SAR distributions over the x-y plane (z = the center of the antenna) for the antenna in the vicinity of the tri-layered model at 1 cm depth in the muscle tissue is given in Fig. 5. The origin of the coordinate system is located at the center of the antenna. The peak SAR of the proposed antenna is 1.32 W/kg and 1.44 W/kg in 434 MHz and 915 MHz, respectively, which is compatible with the regulated SAR limitation (> 0.5 W/kg) of IEEE standard for local hyperthermia applications. As shown in Fig. 5 the SAR penetration has a uniform distribution corresponding to the middle quantities in the biological tissues. Another criterion in hyperthermia application is penetration depth. In local hyperthermia, the penetration depth is defined as the depth at which the SAR becomes $1/e^2$ of its value at the surface. The penetration depths of 6 cm and 6.5 cm are obtained at 434 and 915 MHz, respectively. Normalized measured SAR distribution at 1 cm inside the simulated muscle phantom liquid for the proposed antenna is shown in Fig. 6. Table 3 shows the characteristics of the proposed antenna compared to other designed antennas reported in [12] and [13]. As shown in Table 3, the antenna in [12] has a more compact sized while the peak SAR at two designed frequencies does not satisfy the IEEE standards (SAR > 0.5 W/kg). The planar microstrip antenna reported in [12] has been designed on opposite sides of a dielectric substrate (Rogers Duroid RT5880) with dielectric constant $\varepsilon_r = 2.2$ and thickness of 1.575 mm. The antenna in [13] approximately has the same dimensions as this work, and reported peak SAR is compatible at both frequencies. However in [13], the antenna has no experimental results, and it was designed on a conformal liquid crystal polymer (LCP) substrate. In addition, the proposed antenna in our work is appropriate for flat surface while the antenna in [13] is suitable for conformal surface. In the process of antenna design, two excitation ports with two conformal patches and a silicone oil bolus with an

additional foam layer have been used so that fabrication and design of the antenna became complicated compared to this work. It should be noted that in this work measured return loss and SAR are considered while in [12] and [13] there is no experimental verification of SAR patterns or return loss.

4. CONCLUSION

In this paper we design a low profile dual-band planar antenna for local hyperthermia. The proposed antenna has the advantage of dual-band operation at $f_1 = 434\,\text{MHz}$ and $f_2 = 915\,\text{MHz}$ as well as more compact size ($124 \times 124\,\text{mm}^2$) which makes it a more suitable choice for superficial local hyperthermia. The effect of various gaps between the antenna and the biological tissues is studied in both designed frequencies. In the next step, SAR distribution at 1 cm depth inside the muscle tissue is investigated using simulated muscle phantom liquid return loss and SAR measured. Simulated and measured return losses and SARs show a good electromagnetic performance of the proposed antenna based on IEEE standards.

REFERENCES

1. Wust, P., B. Hildebrandt, G. Sreenivasa, B. Rau, J. Gellermann, H. Riess, R. Felix, and P. M. Schlag, "Hyperthermia in combined treatment of cancer," *The Lancet Oncology*, Vol. 3, No. 8, 487–497, 2002.
2. Van der Zee, J., "Heating the patient: A promising approach," *Annals of Oncology*, Vol. 13, No. 8, 1173–1184, 2002.
3. Vrba, D., D. B. Rodrigues, J. Vrba, Jr., and P. R. Stauffer, "Metamaterial antenna arrays for improved uniformity of microwave hyperthermia treatments," *Progress In Electromagnetic Researche*, Vol. 156, 1–12, 2016.
4. Takook, P., M. Persson, J. Gellermann, and H. D. Trefná, "Compact self-grounded bow-tie antenna design for an UWB phased-array hyperthermia applicator," *Int. J. Hyperthermia*, Vol. 33, No. 4, 2017.
5. Curto, S., P. McEvoy, X. Bao, and M. J. Ammann, "Compact patch antenna for electromagnetic interaction with human tissue at 434 MHz," *IEEE Trans. Antennas Propag.*, Vol. 57, No. 9, 2564–2571, 2009.
6. Hand, J. W., J. L. Cheetham, and A. J. Hind, "Absorbed power distributions from coherent microwave arrays for localized hyperthermia," *IEEE Trans. Microw. Theory Tech.*, Vol. 34, No. 5, 484–489, 1986.
7. Gupta, R. C. and S. P. Singh, "Analysis of the sar distributions in three-layered bio-media in direct contact with a water-loaded modified box horn applicator," *IEEE Trans. Microw. Theory Tech.*, Vol. 53, No. 9, 2665–2671, 2005.
8. Mason, P., W. D. Hurt, T. J. Walters, et al., "Effects of frequency, permittivity, and voxel size on predicted specific absorption rate values in biological tissue during electromagnetic-field exposure," *IEEE Trans. Microw. Theory Tech.*, Vol. 48, No. 11, 2050–2058, 2000.
9. Kim, J. and Y. Rahmat-Samii, "Implanted antennas inside a human body: Simulations, designs, and characterizations," *IEEE Trans. Microw. Theory Tech.*, Vol. 52, No. 8, 1934–1943, 2004.
10. James, J. R. and P. S. Hall, *Handbook of Microstrip Antennas*, Vol. 28, 529–538, IET, 1989.
11. Trefná, H. D., H. Crezee, M. Schmidt, et al., "Quality assurance guidelines for the application of superficial hyperthermia: II. Technical requirements for heating devices," *Strahlentherapie und Onkologie*, Vol. 193, No. 5, 2017.
12. Ali, M. M. M., O. Haraz, I. Elshafiey, S. Alshebeili, and A.-R. Sebak, "Efficient single-band and dual-band antennas for microwave imaging and hyperthermia treatment of brain tumors," *4th IEEE International Conference on Control System, Computing and Engineering (ICCSCE 2014)*, Penang, Malaysia, Nov. 28–30, 2014.
13. Halheit, H., A. V. Vorst, S. Tedjini, and R. Touhami, "Flexible dual frequency applicator for local hyperthermia," *International Journal of Antennas and Propagation*, Vol. 12, 2012.